Multiparameter diagnostic model based on ^{18}F-FDG positron emission tomography and serological examination for differentiating focal autoimmune pancreatitis from pancreatic ductal adenocarcinoma

Guanyun Wang[1,2#], Lei Du[2#], Xia Lu[1], Shengxin Chen[3,4], Xiao Bi[2], Mingyu Zhang[1], Xiaohui Luan[2,3], Xiaodan Xu[2], Zhuochao Zhang[5], Baixuan Xu[2], Jigang Yang[1]

[1]Department of Nuclear Medicine, Beijing Friendship Hospital, Capital Medical University, Beijing, China; [2]Department of Nuclear Medicine, The First Medical Center, Chinese PLA General Hospital, Beijing, China; [3]Graduate School, Chinese PLA General Hospital, Beijing, China; [4]Department of Gastroenterology and Hepatology, The First Medical Center, Chinese PLA General Hospital, Beijing, China; [5]Faculty of Hepato-Pancreato-Biliary Surgery, Chinese PLA General Hospital, Beijing, China

Contributions: (I) Conception and design: G Wang, L Du, B Xu, J Yang; (II) Administrative support: B Xu, J Yang; (III) Provision of study materials or patients: G Wang, L Du, S Chen, X Lu, X Bi; (IV) Collection and assembly of data: G Wang, L Du, S Chen, X Lu, X Bi; (V) Data analysis and interpretation: G Wang, L Du, M Zhang, X Xu, Z Zhang; (VI) Manuscript writing: All authors; (VII) Final approval of manuscript: All authors.

[#]These authors contributed equally to this work.

Correspondence to: Jigang Yang, MD. Department of Nuclear Medicine, Beijing Friendship Hospital, Capital Medical University, 95 Yong'an Road, Xicheng District, Beijing 100050, China. Email: yangjigang@ccmu.edu.cn; Baixuan Xu, MD. Department of Nuclear Medicine, The First Medical Center, Chinese PLA General Hospital, 28 Fuxing Road, Haidian District, Beijing 100853, China. Email: xbx301@163.com.

Background: ^{18}F-fluorodeoxyglucose positron emission tomography-computerized tomography (^{18}F-FDG PET-CT) has demonstrated high sensitivity in the diagnosis of autoimmune pancreatitis (AIP) and pancreatic ductal adenocarcinoma (PDAC), while also exhibiting the ability to distinguish AIP from PDAC lesions. The objective of this investigation was to assess the efficacy of multiparametric ^{18}F-FDG PET with serological examination for distinguishing focal AIP (f-AIP) from PDAC.

Methods: A total of 127 patients (43 with f-AIP and 84 with PDAC) who received ^{18}F-FDG PET-CT before treatment were retrospectively included in the cohort study conducted at two centers, Beijing Friendship Hospital and Chinese PLA General Hospital, from January 2015 to December 2021. The baseline characteristics and clinical data were collected. The metabolism parameters of ^{18}F-FDG PET, including maximum standardized uptake value (SUVmax), tumor-to-normal liver SUV ratio (SUVR), mean SUV (SUVmean), total lesion glycolysis (TLG), and metabolic tumor volume (MTV) were evaluated. The area under the receiver operating characteristic (ROC) curve was used to evaluate the differential diagnostic efficacy. The diagnostic efficacy improvement was assessed through the integrated discriminatory improvement (IDI), net reclassification improvement (NRI), and DeLong test.

Results: Serum immunoglobulin G4 (IgG4) >280 mg/dL, carbohydrate antigen 19-9 (CA19-9) <85 U/mL, and metabolic parameters differed significantly between patients with f-AID and PDAC. The ROC curve analysis of MTV showed the highest differentiating diagnostic value [sensitivity =0.814, 95% confidence interval (CI): 0.661–0.911; specificity =0.893, 95% CI: 0.802–0.947; area under the curve (AUC) =0.890, 95% CI: 0.820–0.957]. The combined diagnostics model of serum IgG4 >280 mg/dL, CA19-9 <85 U/mL, and MTV resulted in the highest AUC of 0.991 (95% CI: 0.978–1.000; sensitivity =0.953, 95% CI: 0.829–0.992; specificity =0.964, 95% CI: 0.892–0.991).

Conclusions: The multiparameter diagnostic model based on ^{18}F-FDG PET and serological examination has excellent clinical value in the differential diagnosis of f-AID and PDAC.

Keywords: Positron emission tomography (PET); focal autoimmune pancreatitis (f-AIP); pancreatic ductal adenocarcinoma (PDAC); metabolic parameters; differential diagnosis

Introduction

Autoimmune pancreatitis (AIP) is a special type of chronic pancreatic disease that is mediated by autoimmunity and may involve the pancreas focally (focal and multifocal type) and diffusely (diffuse type) (1,2). Compared to diffuse AIP, focal AIP (f-AIP), which accounts for 28–48% of all cases of AIP (3), is difficult to from pancreatic ductal adenocarcinoma (PDAC), as their imaging and clinical characteristics often overlap (4,5). Because the treatment of AIP mainly depends on steroids or rituximab (6), and the response is good in most patients (7), PDAC treatment mainly consists of surgery and chemotherapy. Therefore, the differential diagnosis of AIP and PDAC is critical, as this can prevent patients from receiving unnecessary treatment (8). However, the differential diagnosis of pancreatic cancer from AIP is highly challenging in clinical practice because AIP, especially the focal type, can mimic PDAC clinically and radiologically, and vice versa (9-11).

The clinical diagnosis of AIP relies on serological examination, imaging examination, and histopathology examination (12). However, histology is not usually available. Elevated serum immunoglobulin G4 (IgG4) level is highly sensitive to the diagnosis of type 1 AIP, but elevated serum IgG4 level also occurs in some patients with PDAC (13). AIP has characteristic features in contrast-enhanced computerized tomography (CT) and magnetic resonance imaging (MRI) (14); however, in patients with AIP with a focal pancreatic mass, contrast-enhanced CT or MRI may not provide specific information (12). Therefore, it is necessary to find a more effective way to differentiate f-AIP from PDAC.
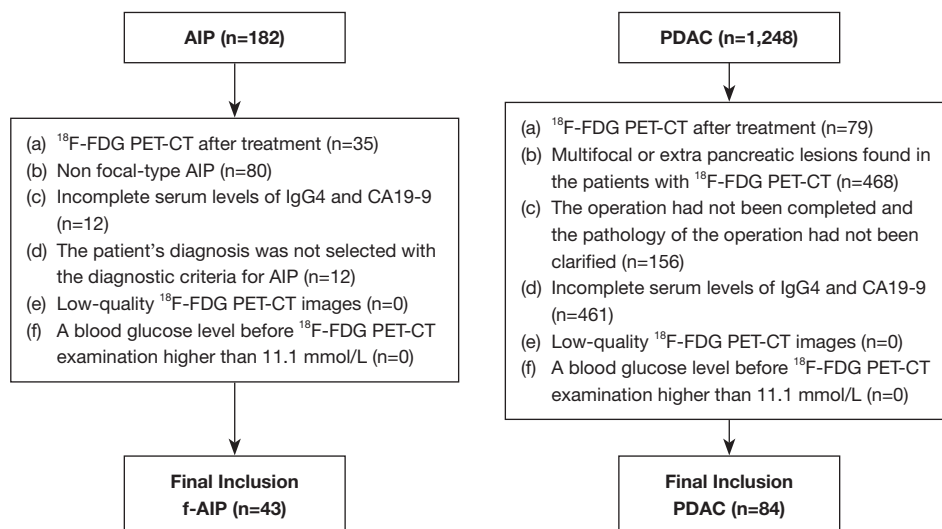
^{18}F-fluorodeoxyglucose positron emission tomography-CT (^{18}F-FDG PET-CT) has been demonstrated to have high sensitivity in the diagnosis of AIP and PDAC and has shown the ability to distinguish AIP from PDAC lesions (15-17). However, no study on the differential diagnosis of f-AIP and PDAC using ^{18}F-FDG PET-CT has been conducted. Hence, this study was initiated to quantitatively compare the lesion contrast between f-AIP and PDA using ^{18}F-FDG PET-CT and to evaluate its diagnostic performance in distinguishing f-AIP from PDAC. We present this article in accordance with the STARD reporting checklist (available at https://qims.amegroups.com/article/view/10.21037/qims-23-88/rc).

Methods

Patients

We retrospectively recruited patients who had undergone ^{18}F-FDG PET-CT before treatment for pancreatic lesions in two centers, Beijing Friendship Hospital and Chinese PLA General Hospital, from January 2015 to December 2021. The patients with f-AIP were diagnosed on the basis of the Revised Japanese Pancreas Society criteria of AIP (18) or the International Consensus Diagnostic Criteria for AIP (12). The following inclusion criteria for the patients with f-AIP were applied: (I) ^{18}F-FDG PET-CT was applied before treatment; (II) the focal type was defined as the presence of a single mass constituting less than half of the total pancreas area in ^{18}F-FDG PET; (III) pretreatment serum levels of IgG4 and carbohydrate antigen 19-9 (CA19-9) were available; and (IV) the patient's diagnosis was made using the diagnostic criteria for AIP. Cases with masses involving more than 50% of the pancreatic area (diffuse type) or multiple masses involving two or more sites (multifocal type) were excluded (3). The following inclusion criteria were applied for patients with PDAC: (I) the ^{18}F-FDG PET-CT was applied before treatment; (II) no multifocal or diffuse lesions on the pancreas or extrapancreatic lesions were found on ^{18}F-FDG PET-CT; (III) the operation had been completed and the pathology of the operation had been clarified; and (IV) pretreatment serum levels of IgG4 and CA19-9 were available. The exclusion criteria for both patients with f-AIP and those

Figure 1 Flow diagram. AIP, autoimmune pancreatitis; PDAC, pancreatic ductal adenocarcinoma; ^{18}F-FDG PET-CT, ^{18}F-fluorodeoxyglucose positron emission tomography-computerized tomography; IgG4, immunoglobulin G4; CA19-9, carbohydrate antigen 19-9; f-AIP, focal AIP.

with PDAC were as follows: (I) low-quality ^{18}F-FDG PET-CT images and (II) a blood glucose level before ^{18}F-FDG PET-CT examination higher than 11.1 mmol/L. The ^{18}F-FDG PET-CT examination and final diagnosis of f-AIP and PDAC were both within 1 month. Finally, we enrolled 43 patients with f-AIP and 84 patients with PDAC who met the criteria from 182 patients with f-AIP and 1,248 patients with PDAC, respectively (*Figure 1*).

The study was conducted in accordance with the Declaration of Helsinki (as revised in 2013) and was approved by ethics review board of Beijing Friendship Hospital of Capital Medical University (No. 2022-P2-321-03) and the ethics review board of Chinese PLA General Hospital (No. S2016-098-01). Individual consent for this retrospective analysis was waived.

Image acquisition

All ^{18}F-FDG PET-CT examinations were conducted in accordance with the guidelines established by the European Association of Nuclear Medicine (EANM) (19). After fasting for at least 4–6 hours, all patients underwent ^{18}F-FDG PET-CT imaging implemented with a Discovery VCT (GE HealthCare, Chicago, IL, USA), Biograph 64 (Siemens Healthineers, Erlangen, Germany), or Biograph mCT (Siemens Healthineers) system. Patients were required to rest in a quiet waiting room for at least 20–30 minutes,

and their blood glucose levels were required to decrease to below 11.1 mmol/L before the intravenous administration of ^{18}F-FDG. ^{18}F-FDG was intravenously administered at a dose of 3.5–4.5 MBq/kg, and images were acquired in free-breathing mode from the skull base or apex of the liver to the upper femur 45–60 minutes after injection. The parameters for low-dose CT (LDCT) were set at a voltage range of 120–140 kV, a current of 100 mAs, a rotation speed of 0.8, a layer thickness between 3 and 5 mm, and a pitch value of 1. PET imaging was conducted in 3D mode with an acquisition time per bed ranging from 2 to 2.5 minutes (30% overlap), 4 to 5 beds per person, 3 iterations, and 21 subsets. The Gaussian filter half-height width was set at a value of 4.0 mm. The images were reconstructed using the ordered subset expectation maximization (OSEM) algorithm with CT attenuation correction (AC).

Image analysis

Two experienced nuclear medicine physicians (WGY and DL, with 5 and 10 years of experience, respectively) interpreted the images using an Advantage Workstation version 4.6 (GE HealthCare) while being blinded to the clinical information of the patients. The physicians arrived at a consensus regarding the interpretation of the imaging findings. The lesions were defined as areas exhibiting abnormal ^{18}F-FDG uptake on PET and/or abnormal

density on CT imaging. 3D volumes of interest (VOIs) were manually delineated around each lesion, with a particular focus on patients with PDAC in whom only focal tumor lesions were manually drawn. The parameters of PET including maximum standardized uptake value (SUVmax), mean SUV (SUVmean), metabolic tumor volume (MTV), total lesion glycolysis (TLG; SUVmean × MTV), tumor-to-normal liver SUV ratio (SUVR; SUVmax of the tumor/ SUVmean of the normal liver parenchyma). Two nuclear medicine physicians measured MTV from attenuation-corrected ^{18}F-FDG PET images in order to obtain these measurements. We used a threshold of 40% of SUVmax to select the pancreatic lesions.

There were some fundamental differences in machine design and scintillation detection among the three PET-CT systems, which could potentially introduce confounding factors into SUVmax measurements to varying degrees (20). To address this issue, we conducted a retrospective analysis to determine the SUVmean of liver parenchyma in 127 patients for whom original PET-CT images were available (GE Discovery VCT: n=51; Siemens Biograph 64: n=48; Siemens Biograph mCT: n=28) (21). To assess the activity of normal liver parenchyma, 3 nonoverlapping spherical VOIs with a volume of 1 cm^3 each were delineated on axial PET images within the normal liver. The SUVmean liver values did not differ significantly among the 3 PET-CT scanners (GE Discovery VCT: 1.97±0.30; Siemens Biograph 64: 1.96±0.33; Biograph mCT: 1.92±0.26; P=0.762, variance analysis).

Statistical analysis

Categorical variables are presented as frequencies and percentages [n (%)] in the form of qualitative data description. The Kolmogorov-Smirnov test was employed to assess the normality of data distribution. For normally distributed continuous variables, an independent samples t-test was used [mean ± standard deviation (SD)] to compare ^{18}F-FDG PET-CT parameters between f-AIP and PDAC, while for skewed continuous variables, the Mann-Whitney test was employed [median (interquartile range)]. The predictive value of PET parameters was evaluated by calculating the area under the receiver operating characteristic (ROC) curve. We computed the sensitivity, specificity, positive predictive value (PPV), and negative predictive value (NPV) in turn. The multivariate logistic regression analysis was employed to develop diagnostic models for discriminating between f-AIP and PDAC. The

DeLong test, integrated discriminatory improvement (IDI), and net reclassification improvement (NRI) were computed to compare diagnostic models and metabolic parameters with the highest area under the curve (AUC). The IDI and NRI were executed using the PredictABEL package in R (The R Foundation for Statistical Computing, Vienna, Austria), while the DeLong test was conducted using the pROC package in R. Patients with missing values were to be excluded, but no patients had missing values. The statistical analysis was conducted using commercially available software, including SPSS 24 (IBM Corp., Armonk, NY, USA) and R version 4.0.2 software. All statistical tests were two-tailed with a significance level set at P=0.05.

Results

Clinical characteristics

A total of 127 patients, including 43 patients with f-AIP and 84 patients with PDAC, were included in the study. Among the 43 patients with f-AIP, 18 obtained pathological results of pancreatic (n=12) or extrapancreatic lesions (n=6), 3 of whom were diagnosed with pancreatic cancer before operation and underwent resection of pancreatic lesions. The clinical characteristics of f-AIP and PDAC are compared in *Table 1*. There was no difference in age or gender distribution between the f-AIP and PDAC groups, but a significant difference was observed in the BMI between the f-AIP and PDAC groups (22.6±3.2 *vs.* 23.9±2.8 kg/m^2, P=0.014). Compared with PDAC, f-AIP occurred more frequently in the head and neck of the pancreas, but there was no significant difference in the size of lesions between the two groups. In the laboratory examination, the value of serum IgG4 [656.0 (291.0–1,100.0) *vs.* 43.8 (20.3–63.6) mg/dL, P<0.001], the proportion of those with serum IgG4 >280 mg/dL [33 (77%) *vs.* 0 (0%), P<0.001], and the proportion of those with CA19-9 <85 U/mL [35 (81%) *vs.* 38 (45%), P<0.001] in the f-AIP group were higher than those in the PDAC group; meanwhile, the value of CA19-9 [101.9 (42.2–305.6) *vs.* 32.7 (9.6–62.1) U/mL, P<0.001] in the PDAC group was higher than that in the f-AIP group.

Comparison of PET metabolic parameters between f-AIP and PDAC

Overall, there were no significant differences between the f-AIP and PDAC groups in SUVmax [5.1 (3.9–6.4) *vs.* 6.3 (4.3–8.6), P=0.062] or SUVR [2.6 (2.2–3.3) *vs.* 2.9

Table 1 Baseline characteristics, imaging data, and laboratory data between the f-AIP and PDAC groups

Characteristics	f-AIP (n=43)	PDAC (n=84)	P value
Age (years)	61.4±11.2	60.4±8.7	0.575
Gender (male:female)	33 [77]:10 [23]	53 [63]:31 [31]	0.120
BMI (kg/m^2)	22.6±3.2	23.9±2.8	0.014
Imaging data			
Lesion size (mm)	32.4±10.3	29.1±10.8	0.093
Location of the lesions			<0.001
Head and neck	35 [81]	41 [49]	
Body and tail	8 [19]	43 [51]	
Laboratory data			
IgG4 (mg/dL)	656.0 (291.0–1,100.0)	43.8 (20.3–63.6)	<0.001
IgG4 >280 mg/dL	33 [77]	0 [0]	<0.001
CA19-9 (U/mL)	32.7 (9.6–62.1)	101.9 (42.2–305.6)	<0.001
CA19-9 <85 U/mL	35 [81]	38 [45]	<0.001

Data are presented as the mean ± SD, median (interquartile range), or n [%]. f-AIP, focal autoimmune pancreatitis; PDAC, pancreatic ductal adenocarcinoma; BMI, body mass index; IgG4, immunoglobulin G4; CA19-9, carbohydrate antigen 19-9; SD, standard deviation.

Table 2 The value of ^{18}F-FDG PET metabolic parameters between the f-AIP and PDAC groups

Variables	f-AIP	PDAC	P value
SUVmax	5.1 (3.9–6.4)	6.3 (4.3–8.6)	0.062
SUVR	2.6 (2.2–3.3)	2.9 (2.1–4.2)	0.113
SUVmean	3.0 (2.3–3.6)	3.3 (2.6–5.0)	0.042
TLG	100.0 (66.3–138.4)	42.2 (30.6–66.9)	<0.001
MTV	33.5 (23.5–48.6)	13.0 (9.3–18.9)	<0.001

Data are presented as the median (interquartile range). ^{18}F-FDG PET, ^{18}F-fluorodeoxyglucose positron emission tomography; f-AIP, focal autoimmune pancreatitis; PDAC, pancreatic ductal adenocarcinoma; SUVmax, maximum standardized uptake value; SUVR, standardized uptake value ratio; SUVmean, mean standardized uptake value; TLG, total lesion glycolysis; MTV, metabolic tumor volume.

(2.1–4.2), P=0.113]. When the threshold method based on 40% of the SUVmax was used, the SUVmean in the f-AIP group was lower than that in the PDAC group [3.0 (2.3–3.6) *vs.* 3.3 (2.6–5.0), P=0.042], but TLG [100.0 (66.3–138.4) *vs.* 42.2 (30.6–66.9), P<0.001] and MTV [33.5 (23.5–48.6) *vs.* 13.0 (9.3–18.9), P<0.001] were higher in the PDAC group (*Table 2*).

### *The differential diagnostic performance of PET metabolic parameters in f-AIP and PDAC*

The diagnostic performance is summarized in *Table 3*

and *Figure 2*. The ROC curve showed that MTV had the highest diagnostic ability among the PET metabolic parameters, the cutoff was 22.4, and the AUC was 0.890 (95% CI: 0.820–0.957). The results showed that the diagnostic accuracy was 87%, the sensitivity was 0.814 (95% CI: 0.661–0.911), the specificity was 0.893 (95% CI: 0.802–0.947), the PPV was 0.795 (95% CI: 0.642–0.897), the NPV was 0.904 (95% CI: 0.814–0.954), and the Youden Index was 0.707. We constructed two diagnostic models based on multivariate logistic regression analysis, including model 1(IgG4 >280 mg/dL plus CA19-9 <85 U/mL) and model 2 (IgG4 >280 mg/dL plus CA19-9 <85 U/mL plus

Table 3 Differential diagnostic efficacies of ^{18}F-FDG PET parameters and different diagnostic models for distinguishing between f-AIP and PDAC

Parameters	Accuracy (%)	Cutoff	AUC (95% CI)	Sensitivity (95% CI)	Specificity (95% CI)	PPV (95% CI)	NPV (95% CI)	Youden index
MTV	87	22.4	0.890 (0.820–0.957)	0.814 (0.661–0.911)	0.893 (0.802–0.947)	0.795 (0.642–0.897)	0.904 (0.814–0.954)	0.707
TLG	76	64.6	0.828 (0.753–0.904)	0.814 (0.661–0.911)	0.726 (0.616–0.815)	0.603 (0.466–0.727)	0.884 (0.779–0.945)	0.540
Model 1	92	–	0.924 (0.868–0.980)	0.767 (0.610–0.877)	1.000 (0.946–1.000)	1.000 (0.870–1.000)	0.893 (0.809–0.945)	0.767
Model 2	96	–	0.991 (0.978–1.000)	0.953 (0.829–0.992)	0.964 (0.892–0.991)	0.931 (0.803–0.982)	0.976 (0.908–0.996)	0.918

Model 1: IgG4 >280 mg/dL plus CA19-9 <85 U/mL; Model 2: IgG4 >280 mg/dL plus CA19-9 <85 U/mL plus MTV. ^{18}F-FDG PET, ^{18}F-fluorodeoxyglucose positron emission tomography; f-AIP, focal autoimmune pancreatitis; PDAC, pancreatic ductal adenocarcinoma; AUC, area under the curve; CI, confidence interval; PPV, positive predictive value; NPV, negative predictive value; MTV, metabolic tumor volume; TLG, total lesion glycolysis; IgG4, immunoglobulin G4; CA19-9, carbohydrate antigen 19-9.
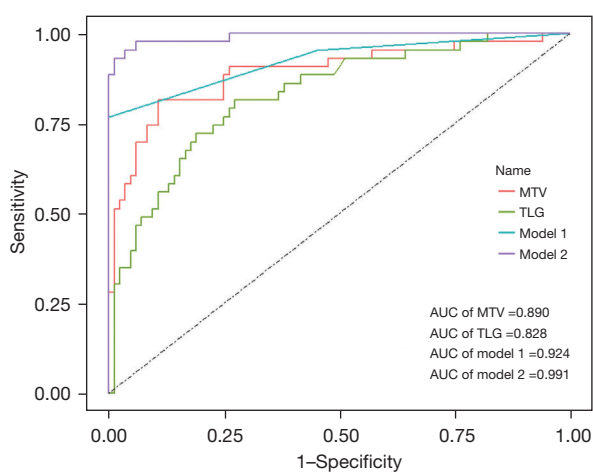
Figure 2 The ROC curves of MTV, TLG, and two different diagnostic models. Model 2 (IgG4 >280 mg/dL plus CA19-9 <85 U/mL plus MTV) demonstrated a high discriminatory ability between f-AIP and PDAC, as evidenced by the AUC of 0.991. Model 1: IgG4 >280 mg/dL plus CA19-9 <85 U/mL; Model 2: IgG4 >280 mg/dL plus CA19-9 <85 U/mL plus MTV. AUC, area under the ROC curve; ROC, receiver operating characteristic; MTV, metabolic tumor volume; TLG, total lesion glycolysis; IgG4, immunoglobulin G4; CA19-9, carbohydrate antigen 19-9; f-AIP, focal autoimmune pancreatitis; PDAC, pancreatic ductal adenocarcinoma.

MTV). Model 1 had an AUC of 0.924 with a Youden index of 0.767, a diagnostic accuracy of 92%, a sensitivity of 0.767 (95% CI: 0.610–0.877), a specificity of 1.000 (95% CI: 0.946–1.000), and a PPV and NPV of 1.000 (95% CI: 0.870–1.000) and 0.893 (95% CI: 0.809–0.945), respectively. Model 2 had an AUC of 0.991 with a Youden index of 0.918, a diagnostic accuracy of 96%, a sensitivity of 0.953 (95% CI: 0.829–0.992), a specificity of 0.964 (95% CI: 0.892–0.991), and a PPV and NPV of 0.931 (95% CI: 0.803–0.982) and 0.976 (95% CI: 0.908–0.996), respectively. Model 2 can be expressed as follows:

$$y = \frac{1}{1 + e^{-(23.55 \times (IgG4 > 280) - 3.39 \times (CA19\text{-}9 < 85) + 0.25 \times MTV - 6.50)}} \quad [1]$$

The comparison between model 2 and the final diagnosis is shown in *Table 4*. Model 2 facilitated a significant reclassification compared to the use of MTV alone (IDI =0.755, 95% CI: 0.671–0.840, P<0.001; NRI categorical =1.277; 95% CI: 1.100–1.454, P<0.001) or model 1 (IDI =0.175, 95% CI: 0.089–0.260, P<0.001; NRI categorical =0.127, 95% CI: 0.010–0.244, P=0.034), respectively. The DeLong test demonstrated that the AUC of model 2 was superior to that of both MTV (Z=3.114, P=0.002) and model 1 (Z=2.630, P=0.009), respectively. The results presented in *Table 5* demonstrate the advantages of using a multiparametric statistical diagnostic approach for distinguishing between f-AIP and PDAC.

Discussion

This study was the first of its kind to identify f-AIP and PDAC by using PET metabolic parameters. We found that ^{18}F-FDG PET metabolic parameters had the ability to distinguish f-AIP from PDAC, and MTV had the best ability to distinguish f-AIP from PDAC. We also developed a diagnostic model based on MTV, IgG4 >280 mg/dL, and CA19-9 <85 U/mL, which significantly enhanced the differential diagnosis of f-AIP from PDAC.

Whether in clinical practice or guidelines, serological examination (including serum IgG4 and CA19-9) is critical in the diagnosis of AIP. Serum IgG4 elevation is the single most salient marker for AIP; however, a portion of patients with PDAC have elevated serum IgG4 levels (22,23); conversely, CA1 9-9 levels are increased in the majority of patients with PDAC, but some patients with AIP have abnormally high CA19-9 levels (24). Although the differential diagnosis ability of serum IgG4 and CA19-9 in f-AIP and PDAC has been confirmed, only one previous study has analyzed the differential diagnosis of f-AIP and PDAC (25). In this study, the combined use of serum IgG4 (>280 mg/dL) and CA19-9 (<85 U/mL) was demonstrated to significantly enhance the diagnostic accuracy of the noninvasive differentiation of pancreatic cancer and AIP, particularly f-AIP (25); the

diagnostic accuracy of f-AIP in pancreatic cancer was reported to reach 85.6%. In our study, the combined use of serum IgG4 (>280 mg/dL) and CA19-9 (<85 U/mL) yielded a higher accuracy rate of up to 92%. However, compared with the abovementioned study, the negative rate of IgG4 in our study was only 23% (vs. 37%), which might have led to an increase in the accuracy of serological examination. The combined use of serum IgG4 (>280 mg/dL) and CA19-9 (<85 U/mL) can effectively differentiate between f-AIP and PDAC, and based on this, IgG4 >280 mg/dL and CA19-9 <85 U/mL were included in our study.

^{18}F-FDG PET is mainly used in patients with PDAC to detect lymph node involvement and metastatic spread at initial staging, as well as to assess and monitor treatment response (26). Moreover, the uptake of FDG has been associated with the aggressiveness of pancreatic tumor in terms of pathological grade (27). However, due to the increase of FDG accumulation in inflammatory lesions (28), this may lead to difficulties in the differential diagnosis of PDAC and pancreatitis, especially focal lesions. Previous studies indicate that ^{18}F-FDG PET-CT may play an important role in displaying pancreatic and extrapancreatic lesions in patients with AIP (15,29), and ^{18}F-FDG PET could distinguish patients with AIP from those with PDAC (15,16,30-32). Ozaki et al. showed that FDG PET is a valuable tool for distinguishing AIP from suspected pancreatic cancer, provided that the accumulation pattern and extrapancreatic involvement are taken into consideration (31). Lee et al. found that the diffuse uptake of FDG by the pancreas or extrapancreatic uptake by the salivary glands on PET-CT could be used to help distinguish AIP from pancreatic cancer (16). Zhang et al. found that the diffuse uptake of FDG in the pancreas could be used to distinguish AIP from pancreatic cancer, and the ^{18}F-FDG PET parameters of pancreas-to-liver SUVR, salivary gland SUV, and prostate SUV may be helpful in distinguishing AIP from pancreatic cancer (15). However,

**Table 4** Comparison between Model 2 and the final diagnosis

Model 2	Final diagnosis, n		
	f-AIP	PDAC	Total
f-AIP	41	3	44
PDAC	2	81	83
Total	43	84	127

Model 2: IgG4 >280 mg/dL plus CA19-9 <85 U/mL plus MTV. f-AIP, focal autoimmune pancreatitis; PDAC, pancreatic ductal adenocarcinoma; IgG4, immunoglobulin G4; CA19-9, carbohydrate antigen 19-9.

Table 5 Comparison of the SUVR and different models according to the DeLong test, IDI, and NRI categorical

Variables	DeLong test		IDI			NRI categorical		
	Z	P	Value	95% CI	P value	Value	95% CI	P value
Model 2 vs. MTV	3.114	0.002	0.755	0.671–0.840	<0.001	1.277	1.100–1.454	<0.001
Model 2 vs. Model 1	2.630	0.009	0.175	0.089–0.260	<0.001	0.127	0.010–0.244	0.034

Model 1: IgG4 >280 mg/dL plus CA19-9 <85 U/mL; Model 2: IgG4 >280 mg/dL plus CA19-9 <85 U/mL plus MTV. SUVR, standardized uptake value ratio; IDI, integrated discrimination improvement; NRI, net reclassification improvement; CI, confidence interval; MTV, metabolic tumor volume; IgG4, immunoglobulin G4; CA19-9, carbohydrate antigen 19-9.

5660

Wang et al. PET and serological examination can differentiate f-AIP from PDAC
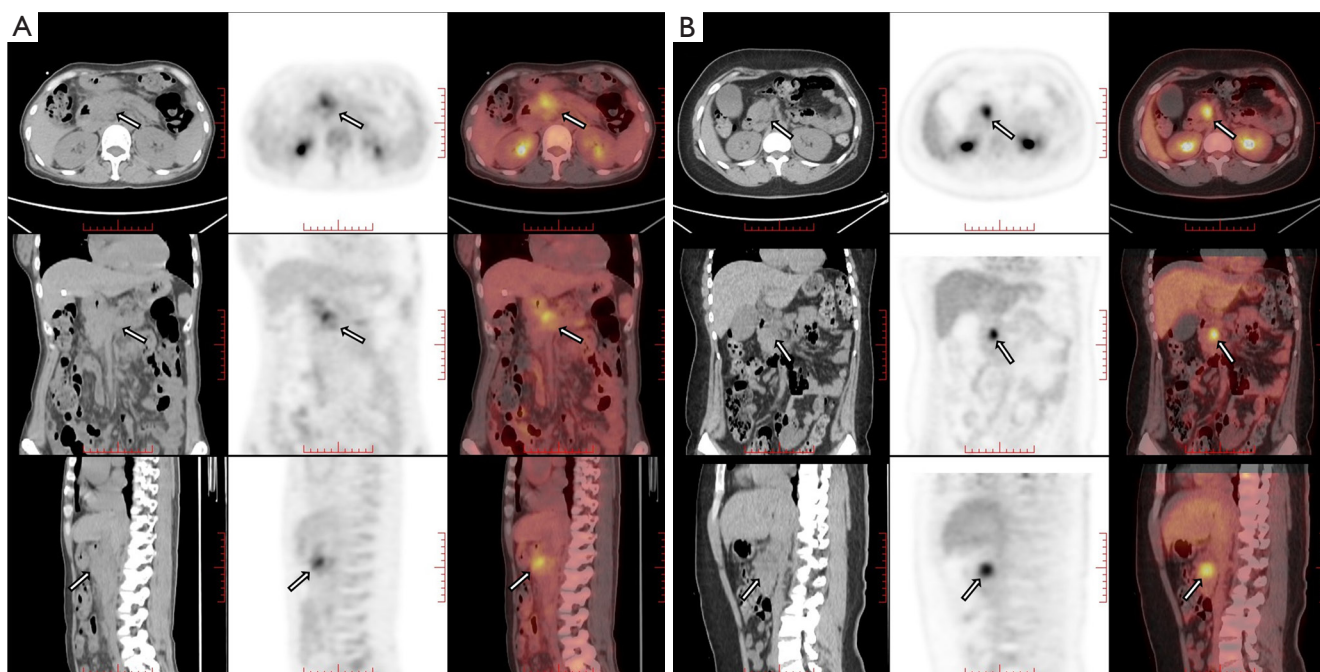
Figure 3 ^{18}F-FDG PET-CT images of patients. (A) Image of a 57-year-old woman with f-AIP in the head of the pancreas (arrows). The serum IgG4 level was 67.4 mg/dL, and the CA19-9 level was 57.3 U/mL. The patient effectively recovered after steroid treatment. The MTV for the lesion was 123.68. (B) Image of a 40-year-old woman with PDAC in the head of the pancreas (arrows). The serum IgG4 level was 78.8 mg/dL, and the CA19-9 level was 1,393.0 U/mL. After surgery, the patient's pathology showed PDAC. The MTV for the lesion was 8.18. ^{18}F-FDG PET-CT, ^{18}F-fluorodeoxyglucose positron emission tomography-computerized tomography; f-AIP, focal autoimmune pancreatitis; IgG4, immunoglobulin G4; CA19-9, carbohydrate antigen 19-9; MTV, metabolic tumor volume; PDAC, pancreatic ductal adenocarcinoma.

using ^{18}F-FDG PET to accurately distinguish inflammatory cells from malignant cells may be difficult because the underlying uptake mechanisms are similar (33), and previous studies did not distinguish between diffuse AIP and f-AIP, reporting that only in conditions of diffuse AIP or abnormal extrapancreatic uptake was the identification of PDAC practicable. For nuclear medicine physicians, distinguishing between f-AIP and PDAC lesions with ^{18}F-FDG PET-CT remains particularly challenging.

Accumulation of ^{18}F-FDG may reflect the metabolic activity of tumors or inflammatory lesions, and volumetric parameters such as MTV represent the volume of lesions with active FDG uptake, which can provide insight into their characteristics (34). Our results showed that MTV had the best differential diagnostic ability in differentiating f-AIP from PDAC among all the ^{18}F-FDG PET metabolic parameters. AIP is a special kind of pancreatitis, which may be related to the infiltration and fibrosis of IgG4-rich lymphoplasmacytes in multiple organs, for which

steroid or other immunomodulatory treatments are usually effective (35). Due to the high glucose metabolism of white blood cells and other inflammatory cells recruited to infected and inflamed tissue, many infectious and inflammatory diseases can be easily detected through ^{18}F-FDG PET-CT (36). However, in our study, we found no difference in SUVmax and SUVR between the f-AIP group and PDAC group. However, compared with PDAC, the inflammatory aggregation range of f-AIP is likely to wider and denser, and so the metabolic volume of FDG represented by MTV may be larger, with PDAC lesions being more limited, FDG uptake being higher, but metabolic volume being smaller (*Figure 3*). This may be the reason why MTV has the highest ability in distinguishing f-AIP from PDAC.

We integrated the differences in serum IgG4 and CA19-9 levels between f-AIP and PDAC, along with the robust diagnostic ability of MTV, to establish a comprehensive diagnostic model. Our own and previous studies suggest that

the combination of serum IgG4 (>280 mg/dL) and CA19-9 (<85 U/mL) have high specificity (1.000, 95% CI: 0.946–1.000), but the sensitivity is relatively low (0.767, 95% CI: 0.6610–0.877). The addition of MTV could compensate for this defect to a certain extent, and the sensitivity (0.953, 95% CI: 0.829–0.992) and specificity (0.964, 95% CI: 0.892–0.991) of the combined model are basically the same. In our study, the application of a combined model significantly improved the differential diagnostic ability compared to using MTV alone, as demonstrated by the IDI, NRI, and DeLong tests. The serum IgG4 (>280 mg/dL) and CA19-9 (<85 U/mL) composite model achieved excellent diagnostic efficiency based on a single metabolic parameter, providing reliable evidence for clinical treatment decisions.

This study had some limitations. First, although this study has the largest number of cases among the relevant studies available and all the patients with PDAC had postoperative pathology. However, some patients with f-AIP did not obtain pathological results. Because f-AIP and PDAC could be distinguished in some patients via clinical and imaging features, invasive pathological examination was not necessary for these f-AIP patients. For patients with f-AIP for whom pathology was not obtained, we screened patients through the guidelines most commonly used in the clinical diagnosis of AIP [the Revised Japanese Pancreas Society criteria of AIP (18) or the International Consensus Diagnostic Criteria (12) for AIP]. Additionally, in order to more accurately select patients with PDAC, we chose patients with complete pathological results via surgery and in whom no metastatic lesions were found in ^{18}F-FDG PET-CT images. Second, because some patients did not have pathological results and the clinical data were incomplete, the type of AIP (type 1 and type 2) was not determined, which could become our focus in future research. Third, most of the patients with f-AIP were diagnosed according to the guidelines, with serology being one of the most important indicators, which might have led to a higher diagnostic efficacy of serological examination than that reported in previous studies. Nonetheless, the diagnostic efficacy was significantly improved after an increase in the metabolic parameters of ^{18}F-FDG PET. Therefore, we believe that the combination model has certain clinical value. Fourth, the SUV is subject to multiple influencing factors (37), which may result in a certain degree of nonreproducibility for the model constructed based on metabolic parameters in diagnosis. Fifth, our study only analyzed patients with PDAC and AIP with focal lesion, so whether a diagnostic model can be used for

patients with metastatic PDAC and patients with diffuse or multifocal AIP still needs to be examined. In the future, we will design prospective studies with a larger sample size to verify the reliability and repeatability of the model and conduct additional analysis by classifying different types of patients. Moreover, we will incorporate PET image omics-related texture parameters to enhance the stability and reproducibility of the model.

Conclusions

In general, the diagnostic model composed of serological examination (including serum IgG4 >280 mg/dL and CA19-9 <85 U/mL) and ^{18}F-FDG PET metabolic parameters (MTV) has excellent diagnostic efficacy in the differential diagnosis of f-AIP and PDAC. Our research can help effectively and accurately identify patients with f-AIP and PDAC and to a certain extent, prevent patients from receiving incorrect or unnecessary treatment due to misdiagnosis.

Acknowledgments

Footnote

Reporting Checklist: The authors have completed the STARD reporting checklist. Available at https://qims.amegroups.com/article/view/10.21037/qims-23-88/rc

Conflicts of Interest: All authors have completed the ICMJE uniform disclosure form (available at https://qims.amegroups.com/article/view/10.21037/qims-23-88/coif). The authors have no conflicts of interest to declare.

Ethical Statement: The authors are accountable for all aspects of the work in ensuring that questions related to the accuracy or integrity of any part of the work are appropriately investigated and resolved. The study was conducted in accordance with the Declaration of Helsinki

(as revised in 2013) and was approved by ethics review board of Beijing Friendship Hospital of Capital Medical University (No. 2022-P2-321-03) and the ethics review board of Chinese PLA General Hospital (No. S2016-098-01). Individual consent for this retrospective analysis was waived.

References

1. Nagpal SJS, Sharma A, Chari ST. Autoimmune Pancreatitis. Am J Gastroenterol 2018;113:1301.

2. de Pretis N, De Marchi G, Frulloni L. Diagnosis and treatment of autoimmune pancreatitis. Curr Opin Gastroenterol 2018;34:362-6.

3. Kwon JH, Kim JH, Kim SY, Byun JH, Kim HJ, Lee MG, Lee SS. Differentiating focal autoimmune pancreatitis and pancreatic ductal adenocarcinoma: contrast-enhanced MRI with special emphasis on the arterial phase. Eur Radiol 2019;29:5763-71.

4. Schima W, Böhm G, Rösch CS, Klaus A, Függer R, Kopf H. Mass-forming pancreatitis versus pancreatic ductal adenocarcinoma: CT and MR imaging for differentiation. Cancer Imaging 2020;20:52.

5. Lopes Vendrami C, Shin JS, Hammond NA, Kothari K, Mittal PK, Miller FH. Differentiation of focal autoimmune pancreatitis from pancreatic ductal adenocarcinoma. Abdom Radiol (NY) 2020;45:1371-86.

6. Hart PA, Topazian MD, Witzig TE, Clain JE, Gleeson FC, Klebig RR, Levy MJ, Pearson RK, Petersen BT, Smyrk TC, Sugumar A, Takahashi N, Vege SS, Chari ST. Treatment of relapsing autoimmune pancreatitis with immunomodulators and rituximab: the Mayo Clinic experience. Gut 2013;62:1607-15.

7. Yoshida K, Toki F, Takeuchi T, Watanabe S, Shiratori K, Hayashi N. Chronic pancreatitis caused by an autoimmune abnormality. Proposal of the concept of autoimmune pancreatitis. Dig Dis Sci 1995;40:1561-8.

8. Kim JH, Kim MH, Byun JH, Lee SS, Lee SJ, Park SH, Lee SK, Park DH, Lee MG, Moon SH. Diagnostic Strategy for Differentiating Autoimmune Pancreatitis From Pancreatic Cancer: Is an Endoscopic Retrograde Pancreatography Essential? Pancreas 2012;41:639-47.

9. Morselli-Labate AM, Pezzilli R. Usefulness of serum IgG4 in the diagnosis and follow up of autoimmune pancreatitis: A systematic literature review and meta-analysis. J Gastroenterol Hepatol 2009;24:15-36.

10. Khandelwal A, Inoue D, Takahashi N. Autoimmune pancreatitis: an update. Abdom Radiol (NY) 2020;45:1359-70.

11. Matsumoto I, Shinzeki M, Toyama H, Asari S, Goto T, Yamada I, Ajiki T, Fukumoto T, Ku Y. A focal mass-forming autoimmune pancreatitis mimicking pancreatic cancer with obstruction of the main pancreatic duct. J Gastrointest Surg 2011;15:2296-8.

12. Shimosegawa T, Chari ST, Frulloni L, Kamisawa T, Kawa S, Mino-Kenudson M, Kim MH, Klöppel G, Lerch MM, Löhr M, Notohara K, Okazaki K, Schneider A, Zhang L; International Association of Pancreatology. International consensus diagnostic criteria for autoimmune pancreatitis: guidelines of the International Association of Pancreatology. Pancreas 2011;40:352-8.

13. Ghazale A, Chari ST, Zhang L, Smyrk TC, Takahashi N, Levy MJ, Topazian MD, Clain JE, Pearson RK, Petersen BT, Vege SS, Lindor K, Farnell MB. Immunoglobulin G4-associated cholangitis: clinical profile and response to therapy. Gastroenterology 2008;134:706-15.

14. Nakazawa T, Ohara H, Sano H, Ando T, Imai H, Takada H, Hayashi K, Kitajima Y, Joh T. Difficulty in diagnosing autoimmune pancreatitis by imaging findings. Gastrointest Endosc 2007;65:99-108.

15. Zhang J, Jia G, Zuo C, Jia N, Wang H. (18)F- FDG PET/CT helps differentiate autoimmune pancreatitis from pancreatic cancer. BMC Cancer 2017;17:695.

16. Lee TY, Kim MH, Park DH, Seo DW, Lee SK, Kim JS, Lee KT. Utility of 18F-FDG PET/CT for differentiation of autoimmune pancreatitis with atypical pancreatic imaging findings from pancreatic cancer. AJR Am J Roentgenol 2009;193:343-8.

17. Shigekawa M, Yamao K, Sawaki A, Hara K, Takagi T, Bhatia V, Nishio M, Tamaki T, El-Amin H, Sayed Zel-A, Mizuno N. Is (18)F-fluorodeoxyglucose positron emission tomography meaningful for estimating the efficacy of corticosteroid therapy in patients with autoimmune pancreatitis? J Hepatobiliary Pancreat Sci 2010;17:269-74.

18. Kawa S, Kamisawa T, Notohara K, Fujinaga Y, Inoue D, Koyama T, Okazaki K. Japanese Clinical Diagnostic

Criteria for Autoimmune Pancreatitis, 2018: Revision of Japanese Clinical Diagnostic Criteria for Autoimmune Pancreatitis, 2011. Pancreas 2020;49:e13-4.

19. Boellaard R, Delgado-Bolton R, Oyen WJ, Giammarile F, Tatsch K, Eschner W, et al. FDG PET/CT: EANM procedure guidelines for tumour imaging: version 2.0. Eur J Nucl Med Mol Imaging 2015;42:328-54.

20. Armstrong IS, Thomson KE, Rowley LM, McGowan DR. Harmonizing standardized uptake value recovery between two PET/CT systems from different manufacturers when using resolution modelling and time-of-flight. Nucl Med Commun 2017;38:650-5.

21. Hsieh CE, Cheng NM, Chou WC, Venkatesulu BP, Chou YC, Liao CT, Yen TC, Lin CY. Pretreatment Primary Tumor and Nodal SUVmax Values on 18F-FDG PET/CT Images Predict Prognosis in Patients With Salivary Gland Carcinoma. Clin Nucl Med 2018;43:869-79.

22. Ghazale A, Chari ST, Smyrk TC, Levy MJ, Topazian MD, Takahashi N, Clain JE, Pearson RK, Pelaez-Luna M, Petersen BT, Vege SS, Farnell MB. Value of serum IgG4 in the diagnosis of autoimmune pancreatitis and in distinguishing it from pancreatic cancer. Am J Gastroenterol 2007;102:1646-53.

23. Ngwa T, Law R, Hart P, Smyrk TC, Chari ST. Serum IgG4 elevation in pancreatic cancer: diagnostic and prognostic significance and association with autoimmune pancreatitis. Pancreas 2015;44:557-60.

24. Yan T, Ke Y, Chen Y, Xu C, Yu C, Li Y. Serological characteristics of autoimmune pancreatitis and its differential diagnosis from pancreatic cancer by using a combination of carbohydrate antigen 19-9, globulin, eosinophils and hemoglobin. PLoS One 2017;12:e0174735.

25. Chang MC, Liang PC, Jan S, Yang CY, Tien YW, Wei SC, Wong JM, Chang YT. Increase diagnostic accuracy in differentiating focal type autoimmune pancreatitis from pancreatic cancer with combined serum IgG4 and CA19-9 levels. Pancreatology 2014;14:366-72.

26. Wartski M, Sauvanet A. 18F-FDG PET/CT in pancreatic adenocarcinoma: A role at initial imaging staging? Diagn Interv Imaging 2019;100:735-41.

27. Ahn SJ, Park MS, Lee JD, Kang WJ. Correlation between 18F-fluorodeoxyglucose positron emission tomography and pathologic differentiation in pancreatic cancer. Ann Nucl Med 2014;28:430-5.

28. Shreve PD. Focal fluorine-18 fluorodeoxyglucose accumulation in inflammatory pancreatic disease. Eur J Nucl Med 1998;25:259-64.

29. Nakajo M, Jinnouchi S, Fukukura Y, Tanabe H, Tateno R, Nakajo M. The efficacy of whole-body FDG-PET or PET/CT for autoimmune pancreatitis and associated extrapancreatic autoimmune lesions. Eur J Nucl Med Mol Imaging 2007;34:2088-95.

30. Cheng MF, Guo YL, Yen RF, Chen YC, Ko CL, Tien YW, Liao WC, Liu CJ, Wu YW, Wang HP. Clinical Utility of FDG PET/CT in Patients with Autoimmune Pancreatitis: a Case-Control Study. Sci Rep 2018;8:3651.

31. Ozaki Y, Oguchi K, Hamano H, Arakura N, Muraki T, Kiyosawa K, Momose M, Kadoya M, Miyata K, Aizawa T, Kawa S. Differentiation of autoimmune pancreatitis from suspected pancreatic cancer by fluorine-18 fluorodeoxyglucose positron emission tomography. J Gastroenterol 2008;43:144-51.

32. Ohtani M, Ofuji K, Akazawa Y, Saito Y, Nosaka T, Ozaki Y, Takahashi K, Naito T, Matsuda H, Hiramatsu K, Nakamoto Y. Clinical Usefulness of [18F]-Fluoro-2-Deoxy-d-Glucose-Positron Emission Tomography/Computed Tomography for Distinguishing Between Autoimmune Pancreatitis and Pancreatic Cancer. Pancreas 2021;50:1014-9.

33. Hess S, Scholtens AM, Gormsen LC. Patient Preparation and Patient-related Challenges with FDG-PET/CT in Infectious and Inflammatory Disease. PET Clin 2020;15:125-34.

34. Hirata K, Tamaki N. Quantitative FDG PET Assessment for Oncology Therapy. Cancers (Basel) 2021;13:869.

35. Khandelwal A, Shanbhogue AK, Takahashi N, Sandrasegaran K, Prasad SR. Recent advances in the diagnosis and management of autoimmune pancreatitis. AJR Am J Roentgenol 2014;202:1007-21.

36. Pijl JP, Nienhuis PH, Kwee TC, Glaudemans AWJM, Slart RHJA, Gormsen LC. Limitations and Pitfalls of FDG-PET/CT in Infection and Inflammation. Semin Nucl Med 2021;51:633-45.

37. Laffon E, Cazeau AL, Monet A, de Clermont H, Fernandez P, Marthan R, Ducassou D. The effect of renal failure on 18F-FDG uptake: a theoretic assessment. J Nucl Med Technol 2008;36:200-2.